

Pretrained Transformers As Universal Computation Engines

Kevin Lu
UC Berkeley
kzl@berkeley.edu

Aditya Grover
Facebook AI Research
adityagrover@fb.com

Pieter Abbeel
UC Berkeley
pabbeel@cs.berkeley.edu

Igor Mordatch
Google Brain
imordatch@google.com

Abstract

We investigate the capability of a transformer pretrained on natural language to generalize to other modalities with minimal finetuning – in particular, without finetuning of the self-attention and feedforward layers of the residual blocks. We consider such a model, which we call a Frozen Pretrained Transformer (FPT), and study finetuning it on a variety of sequence classification tasks spanning numerical computation, vision, and protein fold prediction. In contrast to prior works which investigate finetuning on the same modality as the pretraining dataset, we show that pretraining on natural language can improve performance and compute efficiency on non-language downstream tasks. Additionally, we perform an analysis of the architecture, comparing the performance of a random initialized transformer to a random LSTM. Combining the two insights, we find language-pretrained transformers can obtain strong performance on a variety of non-language tasks¹.

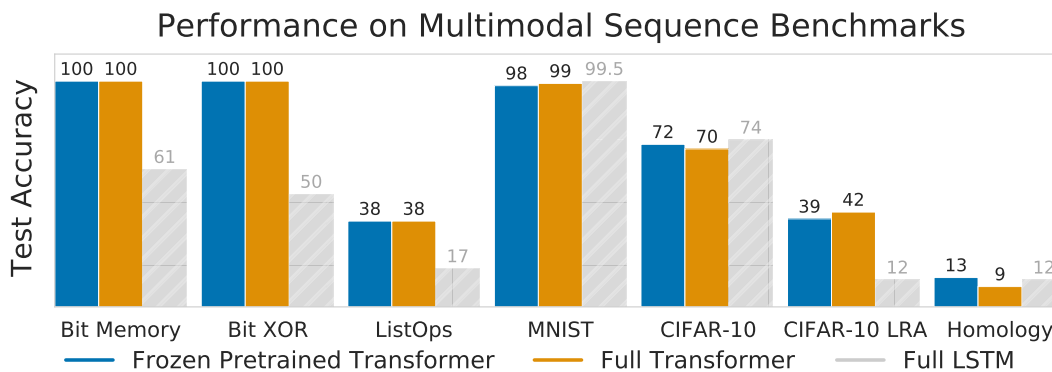


Figure 1: A *frozen* language-pretrained transformer (FPT) – without finetuning the self-attention and feedforward layers – can achieve strong performance compared to a transformer fully trained from scratch on a downstream modality on benchmarks from literature (Tay et al., 2020; Rao et al., 2019). We show results on diverse classification tasks (see Section 2.1): numerical computation (Bit Memory/XOR, ListOps), image classification (MNIST, CIFAR-10), and protein fold prediction (Homology). We also show results for a fully trained LSTM to provide a baseline.

¹Code available at github.com/kzl/universal-computation. For a summary of changes made in the updated arXiv version, see Appendix A.

Contents

1	Introduction	3
2	Methodology	3
2.1	Tasks	3
2.2	Architecture	4
3	Empirical Evaluations	5
3.1	Can pretrained language models transfer to different modalities?	5
3.2	What is the importance of the pretraining modality?	6
3.3	How important is the transformer architecture compared to LSTM architecture?	7
3.4	Does language pretraining improve compute efficiency over random initialization?	8
3.5	Do the frozen attention layers attend to modality-specific tokens?	8
3.6	Does freezing the transformer prevent overfitting or underfitting?	9
3.7	Does performance scale with model size?	9
3.8	Can performance be attributed simply to better statistics for initialization?	10
3.9	Can we train a transformer by only finetuning the output layer?	10
3.10	What is the role of model depth in token mixing?	11
3.11	Can training more parameters improve performance?	11
3.12	Which parameters of the model are important to finetune?	12
3.13	Is finetuning layer norm necessary for FPT to perform well?	12
3.14	How well do the trends hold across other transformer models?	13
4	Related Work and Discussion	13
4.1	Transformers in multimodal settings	13
4.2	Transformers in transfer settings	13
4.3	Pretraining and finetuning of transformer models	14
4.4	Self-attention layers as optimization steps	14
4.5	Global workspace theory	14
4.6	Reservoir computing	15
5	Conclusion	15
	Acknowledgements	15
	References	20
	Appendix	21

1 Introduction

The transformer architecture (Vaswani et al., 2017) has shown broad successes in deep learning, serving as the backbone of large models for tasks such as modeling natural language (Brown et al., 2020), images (Dosovitskiy et al., 2020), proteins (Jumper et al., 2021), behaviors (Abramson et al., 2020), and multimodal tasks comprising of both images and text (Lu et al., 2019; Radford et al., 2021). Inspired by these successes, we seek to explore the generalization capabilities of a transformer in transferring from one modality to another.

Classical approaches to sequence processing used recurrent neural network (RNN) approaches (Rumelhart et al., 1985; Hochreiter & Schmidhuber, 1997). In contrast, transformers utilize self-attention layers to extract features across tokens of a sequence, such as words (Vaswani et al., 2017) or image patches (Dosovitskiy et al., 2020). Furthermore, it has become common practice to train large models on unsupervised or weakly supervised objectives before finetuning or evaluating zero-shot generalization on a downstream task. However, the downstream tasks that have been studied are generally restricted to the same modality as the original training set: for example, train GPT (Radford et al., 2018) on a large language corpus, and finetune on a small task-specific dataset. Our goal in this work is to investigate finetuning on modalities distinct from the training modality.

We hypothesize that transformers, namely the self-attention layers, can be pretrained on a data-rich modality (i.e. where data is plentiful, such as a natural language corpus) and identify feature representations that are useful for *arbitrary* data sequences, enabling downstream transfer to different modalities. In particular, we seek to investigate what pretrained language models (LMs) are capable of in terms of generalizing to other modalities with sequential structure.

To investigate this hypothesis, we take a transformer model pretrained on natural language data, GPT-2 (Radford et al., 2019), and finetune only the linear input and output layers, as well as the positional embeddings and layer norm parameters. We call this model a Frozen Pretrained Transformer (FPT). On a range of tasks across a variety of modalities – including numerical computation, image classification, and protein fold prediction – FPT displays comparable performance to training the entire transformer or LSTM models from scratch, matching reported benchmarks for these tasks (Figure 1). Additionally, we find FPT models also converge faster during training. Our results suggest the self-attention layers learned by a language model may have properties amenable to efficient universal computation. Through a series of experiments, we seek to investigate what contributes to the performance of FPTs by isolating various sub-components of these models.

2 Methodology

2.1 Tasks

We evaluate on a diverse set of classification tasks representative of different modalities. In particular, we are interested in if language models are inherently capable of *universal computation*, by which we mean the ability to learn representations for predictive learning across diverse modalities.

Bit memory. Similar to the task proposed by Miconi et al. (2018), we consider a bit memory task where the model is shown 5 bitstrings each of length 1000. Afterwards, the model is shown a masked version of one of the bitstrings, where each bit is masked with probability 0.5, and the model is tasked with producing the original bitstring. The bitstrings are broken up into sequences of length 50, so that the models are fed 120 tokens of dimension 50.

Bit XOR. Similar to the bit memory task, the model is shown 2 bitstrings of length 5, where the model must predict the element-wise XOR of the two bitstrings. The bitstrings are shown 1 bit at a time, so the models are fed 10 tokens of dimension 1.

ListOps. Taken from Tay et al. (2020), the model is shown a sequence of list operations (ex. [MAX 4 3 [MIN 2 3] 1 0]) and tasked with predicting the resulting output digit (ex. 4). This task evaluates the ability of a model to parse mathematical expressions and evaluate over a long context. The model is shown 1 token at a time, so the models are fed 512 tokens of dimension 15.

MNIST. We use the standard MNIST benchmark, where the model must classify a handwritten digit from a 32×32 black-and-white image. The tokens given to the model are 4×4 image patches, so the models are fed 64 tokens of dimension 16.

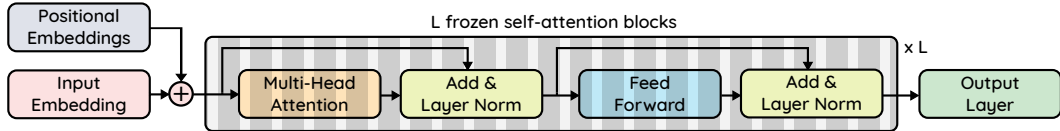


Figure 2: Frozen Pretrained Transformer (FPT). The self-attention & feedforward layers are frozen.

CIFAR-10. We use the standard CIFAR-10 benchmark (Krizhevsky et al., 2009), where the tokens given to the model are 4×4 image patches, so the models are fed 64 tokens of dimension 16.

CIFAR-10 LRA. This is a modified version of the above task taken from the Long Range Arena benchmark where the images are converted to grayscale and flattened with a token length of 1 (Tay et al., 2020). As a result, the input sequence consists of 1024 tokens of dimension 1. This task is much more challenging than vanilla CIFAR-10 classification above as the models must learn patterns over a significantly longer sequence length and have minimal spatial inductive bias.

Remote homology detection. In this task, we are interested in predicting the fold for a protein, represented as an amino acid sequence. We use the datasets provided by TAPE (Rao et al., 2019; Fox et al., 2013; Hou et al., 2018), where the train/test split is generated by holding out certain evolutionary groups. Note that we do not pretrain on Pfam (El-Gebali et al., 2019), which is common in other works. There are 20 common and 5 uncommon amino acids (25 different types of inputs), and there are 1195 possible labels to predict. We only consider sequences of length less than 1024 for simplicity. The models are thus fed up to 1024 tokens of dimension 25.

2.2 Architecture

The architecture we use is summarized in Figure 2. Denote the embedding size/hidden dimension of the transformer as n_{dim} , the number of layers as n_{layers} , (note $n_{dim} = 768$ and $n_{layers} = 12$ for the base size models), the input dimension as d_{in} , the output dimension (number of classes) as d_{out} , and the maximum length of the sequence as l . We consider finetuning the following parameters of a pretrained GPT-2 model (Radford et al., 2019):

- **Output layer:** it is crucial to finetune the output layer since we are transferring to a completely new task – we use the simplest possible instantiation of an output network, being a single linear layer applied to the last output token output by the transformer, in order to highlight that almost all the computation is being performed by the frozen transformer. The output layer has $n_{dim} \times d_{out}$ parameters for the weight matrix. For example, for the base models on CIFAR-10, this comes out to $768 \cdot 10 = 7680$ parameters.
- **Input layer:** it is important to reinitialize a new input layer since we are reading in a new modality; in essence, we are learning how to query the transformer. This contrasts with prior unsupervised embedding evaluation techniques, such as linear probing – due to the change in modality, we instead should train the input layer as well, and evaluate if the frozen intermediate transformer model performs effective computation. Again, we use a linear layer to minimize the amount of computation outside the transformer. The input layer has $d_{in} \times n_{dim}$ parameters for the weight matrix/embeddings, and an additional n_{dim} parameters if there is a bias term. For the base models on CIFAR-10, this comes out to $16 \cdot 768 = 13056$ parameters.
- **Layer norm parameters:** as is standard practice in other finetuning works (Rebuffi et al., 2017; Housby et al., 2019), we also finetune the affine layer norm parameters (scale and bias), which adapt to the statistics of the downstream task in a new domain. In GPT-2, layer norm is applied twice per block, so these are a total of $4 \times n_{dim} \times n_{layers}$ parameters. For the base models on CIFAR-10, these come out to $4 \cdot 768 \cdot 12 = 36684$ parameters.
- **Positional embeddings:** While we observe that positional embeddings can be surprisingly universal between modalities (see Section 3.12), we generally see a small benefit to finetuning the positional embeddings which have a cheap parameter cost of $l \times n_{dim}$. For the base models on CIFAR-10, these come out to $64 \cdot 768 = 49512$ parameters.

Given the cheap linear scaling of these parameters, the parameter counts of large transformer models are dominated by the quadratic (in n_{dim} and l) self-attention and feedforward layers. For the base CIFAR-10 model with 124M parameters, these come out to approximately 0.086% of the network. Due to this scaling, this number decreases with larger model sizes, down to 0.029% of the GPT-2 XL model. We further ablate the importance of each parameter in Section 3.12. For more details and a description of the architecture, see Appendix B.

Note that, crucially, all communication between tokens in the model are frozen. The data in each datapoint is chunked into discrete tokens (bits, image patches, amino acids, etc.), and can only reference each other via the frozen attention connections, which are not trained; additionally, neither the output nor the input layers are connected to multiple tokens. Our key investigation is to analyze the computation that is already inherent in the language model, and hence we do a minimal amount of computation that is learned on the downstream modality.

3 Empirical Evaluations

In this section, we review the results demonstrating transfer from language to other modalities, and seek to better understand why this occurs and what enables this transfer. All model sizes are the base model size (12 layers, 768 hidden dimension), unless stated otherwise. See Appendix C for more details on experiments.

3.1 Can pretrained language models transfer to different modalities?

We investigate if the self-attention and feedforward layers – the main body – of a pretrained transformer can be applied to a classification problem in a different modality without finetuning. To do this, we apply our base procedure as described above, where the input embedding layer, output readout layer, and layer norm parameters are finetuned.

Our results are shown in Figure 1 and also summarized below in Table 1. We compare to state-of-the-art from literature when available (full transformer on ListOps, CIFAR-10 LRA, and Remote Homology; LSTM on Remote Homology). Note the benchmarks from literature do not include decimal points, so for those numbers we report without a decimal.

We find that across all seven tasks considered, FPT achieves comparable performance to the fully trained transformer benchmarks. We believe these results support the idea that these models are learning representations and performing computation that is agnostic to the modality. We also note that both transformer variants significantly outperform LSTMs on some tasks, particularly ListOps and CIFAR-10 LRA, which have long sequence lengths of 512 and 1024, respectively.

On the two bit tasks (Memory and XOR), the models achieve 100% performance, i.e. they are able to recover the exact algorithm. Although our tables show results for $n = 5$, we actually find FPT can still recover the exact algorithm on sequence lengths greater than $n = 256$ (the elementwise XOR of two bitstrings each of length 256), hinting that FPT has a fairly large working memory.

Model	Bit Memory	XOR	ListOps	MNIST	CIFAR-10	C10 LRA	Homology
FPT	100%	100%	38.4%	98.0%	72.1%	38.6%	12.7%
Full	100%	100%	38%	99.1%	70.3%	42%	9%
LSTM	60.9%	50.1%	17.1%	99.5%	73.6%	11.7%	12%

Table 1: Test accuracy of FPT vs fully training transformer on downstream task vs fully training LSTM on downstream task (results are transcribed from Figure 1).

We highlight a few important points for contextualizing these results. We find that it can be difficult to fully train a 12-layer transformer on some of these (relatively small) datasets, as training can either diverge/overfit or be unstable. For CIFAR-10, we report the full transformer results for a 3-layer model; for ListOps and CIFAR-10 LRA we report the number given for the 3-layer model from Tay et al. (2020); for Remote Homology we report the number for a smaller 12-layer model from Rao et al. (2019). From an engineering perspective, this makes the full transformers harder to tune since we must choose model sizes that are stable and avoid overfitting – see Section 3.6 for more

analysis. In particular, the numbers from Tay et al. (2020) are generated from “extensive sweeps over different hyper-parameters” and use task-specific hyperparameters, while we do not tune the hyperparameters for FPT (except for remote homology; see Appendix C). In contrast, we find it is easy to improve the performance of FPT by increasing model size (see Section 3.7) – the CIFAR-10 number for FPT here is for the 36-layer large model.

Furthermore, unlike some other works utilizing transformers for vision, we use minimal spatial bias to emphasize the universal sequential aspect of the problem – for instance, we do not interleave self-attention and convolution layers. Note that we also do not use 2D positional embeddings (or other domain-specific techniques), hence providing very weak inductive prior to the model. Our reasoning for these decisions is to evaluate the ability of transformers to work on arbitrary sequential tasks.

3.2 What is the importance of the pretraining modality?

We now compare pretraining on language to other pretraining methods for base model sizes:

- Random initialization (Random): initialization of the frozen transformer parameters randomly using the default initialization choices for GPT-2, i.e. without pretraining.
- Bit memory pretraining (Bit): pretraining from scratch on the Bit Memory task and then freezing the parameters before transferring. This allows the transformer to gain supervision working with arbitrary bit strings and performing memory/denoising on independent inputs.
- Image pretraining (ViT): using a pretrained Vision Transformer (Dosovitskiy et al., 2020) pretrained on ImageNet-21k (Deng et al., 2009). Note that the architecture is a bit different, notably not using the autoregressive masking of GPT-2, since ViT is only pretrained on classification tasks (for other details, see Appendix D.2).

These experiments highlight the significance of pretraining – as opposed to simply the transformer architecture – and compare language to other methods of supervision. Our results are shown in Table 2. Although the random transformers can achieve surprisingly strong accuracies, there is a considerable gap to using natural language pretraining, such as in MNIST, where random transformers achieve similar performance to a linear classifier on top of raw features (92%). Thus we believe that while the transformer architecture might be naturally conducive to these evaluations, the attention mechanisms used to transfer may be nontrivial and not fully specified by the architecture. We also find that, in addition to performance benefits, language pretraining improves convergence compared to the randomly initialized transformer (see Section 3.4).

Model	Bit Memory	XOR	ListOps	MNIST	C10	C10 LRA	Homology
FPT	100%	100%	38.4%	98.0%	68.2%	38.6%	12.7%
Random	75.8%	100%	34.3%	91.7%	61.7%	36.1%	9.3%
Bit	100%	100%	35.4%	97.8%	62.6%	36.7%	7.8%
ViT	100%	100%	37.4%	97.8%	72.5%	43.0%	7.5%

Table 2: Test accuracy of language-pretrained (FPT) vs randomly initialized (Random) vs Bit Memory pretraining (Bit) vs pretrained Vision Transformer (ViT) models. The transformer is frozen.

Pretraining on bit memory improves performance compared to the random models, but still lags behind training on natural language data. Furthermore, measured by gradient steps, all models converge faster than the randomly initialized transformers (more details in Section 3.4), indicating that all modes of pretraining improve upon random initialization even without considering accuracy.

Additionally, while freezing a vision transformer yields better improvements on CIFAR-10, pretraining on images is not uniformly better; e.g., ViT is worse on protein classification. One hypothesis is that protein sequences are structured like language, in terms of discrete units of information with a “grammar”, so transfer from language to proteins may be more natural.

3.3 How important is the transformer architecture compared to LSTM architecture?

In Section 3.2 we found the transformer architecture can already be fairly effective in this regime, even with only random parameters. In this section, we consider using a random LSTM architecture instead of the transformer, allowing us to consider the raw effect of architecture and ablating pretraining. Like FPT, we finetune the input, output, and layernorm parameters for the LSTMs.

Model	Bit Memory	XOR	ListOps	MNIST	CIFAR-10	C10 LRA	Homology
Trans.	75.8%	100%	34.3%	91.7%	61.7%	36.1%	9.3%
LSTM	50.9%	50.0%	16.8%	70.9%	34.4%	10.4%	6.6%
LSTM*	75.0%	50.0%	16.7%	92.5%	43.5%	10.6%	8.6%

Table 3: Test accuracy of randomly initialized transformers vs randomly initialized LSTM models. Note unlike in Figure 1, the LSTM here is frozen. Frozen LSTMs perform very poorly. LSTM* represents an LSTM with additional architecture improvements to match the transformers (see below).

Our results are shown in Table 3. “LSTM” refers to a 3-layer “standard” LSTM with a hidden dimension of 768, matching standard implementations of LSTMs, without residual connections or positional embeddings (see discussion below). This matches the width of the FPT models, but not the depth or total parameter count (note that LSTMs also do not have positional embeddings). We find that the self-attention architecture already serves as an effective inductive bias for universal computation, improving significantly over the recurrent LSTM model and comprising most of the improvement in test accuracy from random LSTM to FPT.

Here, we compare the 3-layer “standard” LSTM to a 12-layer “standard” LSTM. Note that most LSTM implementations, including the one used in Table 3, do not feature residual connections and positional embeddings. We include this comparison to represent the traditional method more faithfully, but add these additional architectural components below. In the same style of FPT and GPT-2, we do not use a bidirectional LSTM. Under these model choices, we report the performance of a frozen random 3-layer vs 12-layer LSTM in Table 4. Naively, the 12-layer model is much worse than the 3-layer model, hinting that there is some loss of information by repeated LSTM layers.

Layers	ListOps	MNIST	CIFAR-10	C10 LRA
12	16.2%	11.7%	10.8%	10.4%
3	16.8%	70.9%	34.4%	10.4%

Table 4: Test accuracy of randomly initialized “standard” LSTMs varying number of layers with a hidden dimension of 768. The simple 12-layer LSTM achieves only near-trivial performance.

We also experiment with ablating other architectural improvements included with the transformer architecture in Table 5. Once residual connections (He et al., 2016) are added, the 12-layer LSTM makes up a lot of the performance drops, hinting that residual connections could make up for loss of information from the LSTM layers which otherwise linearly combine the features. We also add positional embeddings, which finishes bridging the gap between standard LSTM implementations and the transformer. Even with these additional benefits, the LSTM still performs worse. Note that the final 12-layer LSTM has about the same number of trainable parameters as the transformer.

Model	ListOps	MNIST	CIFAR-10	C10 LRA
12-Layer LSTM	16.2%	11.7%	10.8%	10.4%
+ Residual Connections	16.8%	70.9%	34.4%	10.4%
+ Positional Embeddings	16.7%	92.5%	43.5%	10.6%
Random Transformer	34.3%	91.7%	61.7%	36.1%

Table 5: Test accuracy of 12-layer randomly initialized “standard” LSTMs additional architectures modifications to match transformers: residual connections and positional embeddings. The bottom row, LSTM with residual connections and positional embeddings, is nearly identical to GPT-2.

3.4 Does language pretraining improve compute efficiency over random initialization?

We investigate compute efficiency by considering the number of gradient steps to converge for FPT vs random transformer models, shown in Table 6. We generally find FPT converges faster, which indicates language pretraining can yield compute benefits for non-language tasks. While random transformer models achieve decent test accuracies, in particular when compared to random LSTMs, there is still a considerable gap in the compute efficiency compared to using pretraining. Note that bit memory pretraining introduced in Section 3.2 generally falls between the two models, and notably is $6\times$ slower than FPT on Bit XOR, which is significantly better than random.

Model	Memory	XOR	ListOps	MNIST	C10	C10 LRA	Homology
FPT	1×10^4	5×10^2	2×10^3	5×10^3	4×10^5	3×10^5	1×10^5
Random	4×10^4	2×10^4	6×10^3	2×10^4	4×10^5	6×10^5	1×10^5
Speedup	4x	40x	3x	4x	1x	2x	1x

Table 6: Approximate number of gradient steps until convergence for pretrained (FPT) vs randomly initialized (Random) models. Note that we use the same batch size and learning rate for both models.

3.5 Do the frozen attention layers attend to modality-specific tokens?

We investigate if FPT attends to semantically meaningful patterns in the data. We plot the attention weights (i.e. the values of the softmax of query-key dot product) from the first layer. We show the results in Figures 3 and 4 for the bit tasks. Note GPT-2 is autoregressive, so the upper right corner of the attention mask is zeroed out. On these tasks, FPT yields an interpretable attention pattern despite not training the self-attention layers themselves. We did not find easily interpretable patterns on the other tasks.

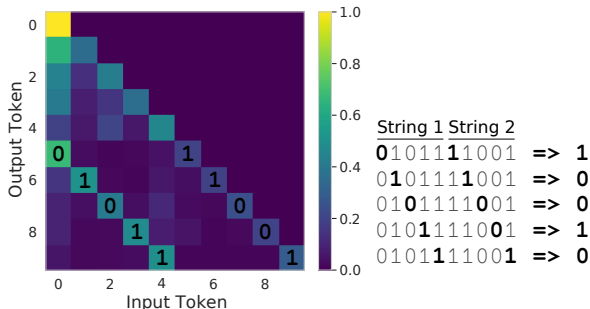


Figure 3: On Bit XOR, the model must produce the element-wise XOR of two bitstrings presented sequentially (inputs 0-4 are the first bitstring, inputs 5-9 are the second). Each token is one bit. FPT learns to attend positionally to the two bits that are XOR’ed by the output token.

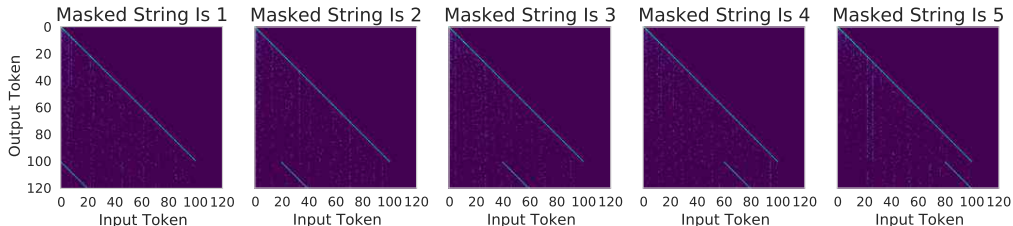


Figure 4: On Bit Memory, the model must return one of five strings (inputs 0-99) given a masked version of one of the strings (inputs 100-119). Each token is 50 bits. FPT learns to attend to the correct string based on finding similarity to the inputs, not relying solely on position as in Bit XOR.

We also include the attention map for Bit XOR using a randomly initialized transformer (which also solves the task) in Figure 5. This model also learns to exploit the diagonal pattern, although the strength is a little weaker. This indicates that while the random transformer still learns to solve the task, it learns a less semantically interpretable/strong attention pattern.

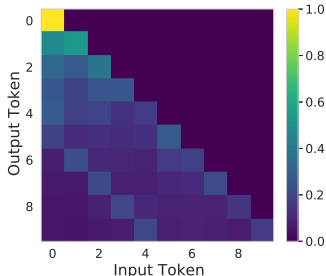


Figure 5: A transformer with frozen randomly initialized self-attention layers also learns to correlate the two diagonal elements on Bit XOR, although the magnitude of the diagonals is lower (note the extra attention weights distributed in between the diagonals).

3.6 Does freezing the transformer prevent overfitting or underfitting?

Our general findings are that – in contrast to their fully trained counterparts – FPT models underfit the data, which lends them to further improvements by increasing model capacity (see Section 3.7). For example, consider CIFAR-10 LRA, which is maximally difficult due to lack of inductive prior over the sequence (each pixel is fed in as an arbitrary token only ordered by a raster scan) and relatively small dataset (50k images). In Table 7, we show the train/test gap between training FPT vs a 3-layer transformer from Tay et al. (2020), which we find to give stronger results than our experiments. In particular, they are much better than training a 12-layer transformer, which works poorly. Our results indicate that FPT is generally providing generalizable task representations without causing overfitting, whereas transformers can overfit arbitrarily poorly in low-data regimes (such as for Linformer, which overfit the most out of the architectures tested by Tay et al. (2020)). More work can investigate how to increase the model expressiveness, which could yield performance benefits.

Model	# Layers	Test Accuracy	Train Accuracy
FPT (GPT-2)	12	38.6%	38.5%
Vanilla Transformer	3	42%	70%
Linformer	3	39%	97%

Table 7: Train vs test accuracies on CIFAR-10 LRA task.

3.7 Does performance scale with model size?

We evaluate the efficacy of adding more parameters to these models on CIFAR-10. Most of the additional parameters are in the transformer layers and are trained during the natural language pre-training phase. Our results for pretrained and random models are in Table 8. Unlike fully training a transformer, which exhibits more overfitting and divergence during training with larger models, increasing model size stably increases the capacity of the models. This result indicates our observations and results are likely to scale as we move towards larger models and higher-data regimes.

Model Size	# Layers	Total Params	Trained Params	FPT	Random
Small (Base)	12	117M	106K	68.2%	61.7%
Medium	24	345M	190K	69.8%	64.0%
Large	36	774M	300K	72.1%	65.7%

Table 8: Test accuracy of larger frozen transformer models on CIFAR-10.

3.8 Can performance be attributed simply to better statistics for initialization?

In this section, we ablate taking the layer-wise mean and standard deviation from the pretrained model and using it to initialize a random transformer, in order to ablate if a better initialization scheme via an “oracle” standard deviation can recover the performance of FPT. Note that the GPT-2 initialization scheme initializes parameters as Gaussian; traditionally, the standard deviation is 0.02 by default. For clarity, we show the standard deviation by layer for the weights and biases of the attention and feedforward layers in Figure 6 for the pretrained models.

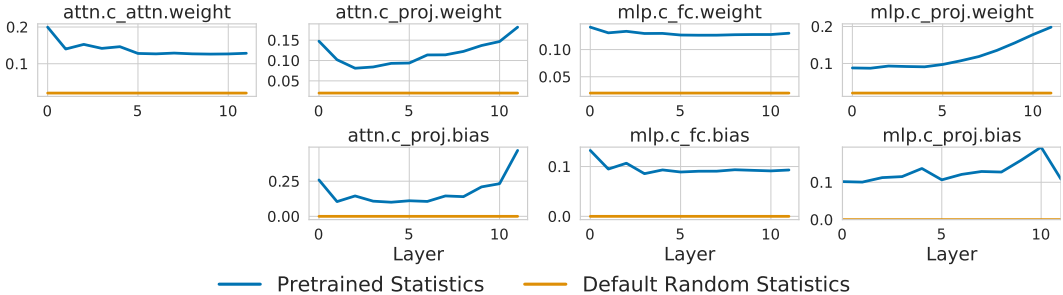


Figure 6: Standard deviation of the parameters by layer for the pretrained GPT-2 model versus default initialization hyperparameters (0.02 for weights and 0 for biases).

We show the results using this initialization scheme in Table 9 (note that all of the weights, biases, layer norm, and positional embeddings are initialized – both mean and variance – in this fashion). This yields better results on most tasks, but does poorly on CIFAR-10. As a result, we believe the benefits of language pretraining cannot be recovered with a simple better initialization scheme, although we believe future work in transformer initialization could yield different results.

Initialization	Memory	XOR	ListOps	MNIST	C10	C10 LRA	Homology
Pretrained	100%	100%	38.4%	98.0%	68.2%	38.6%	12.7%
Statistics Only	100%	100%	37.4%	97.2%	56.5%	33.1%	11.0%
Default	75.8%	100%	34.3%	91.7%	61.7%	36.1%	9.3%

Table 9: Test accuracy when initializing parameters with pretrained weights (i.e., FPT) vs randomly initializing parameters according to the mean and variance of the pretrained transformer (Statistics Only) vs random initialization with default parameters (Default).

3.9 Can we train a transformer by only finetuning the output layer?

We consider using FPT solely for naive feature extraction for linear classification, where we fix a randomly initialized input layer and freeze all parts of the model except for the output. Note that this resembles reservoir computing/echo state networks (see Section 4.5 for discussion). The model evaluates on every example in the training set once, caches the features, and then we train a linear output layer. This enables subsequent epochs after the first to run extremely quickly, but does not easily handle dropout/data augmentations, and scales well in terms of number of epochs, but not in dataset size. Note that this is mathematically equivalent to linear classification. Our results are shown in Table 10. Although we find speedups extremely significant and they obtain nontrivial performance, performance significantly degrades and the models also exhibit overfitting (likely due to lack of regularization; unlike the training of FPT, dropout is not applied).

Task	Speedup	Output Only	FPT	Full Transformer
ListOps	500 – 2000×	32.8%	38.4%	38%
CIFAR-10 LRA	500 – 2000×	24.7%	38.6%	42%

Table 10: Training only the output layer as a linear regression problem. Speedup refers to wall clock time per epoch (after the first). Larger models have larger speedups.

3.10 What is the role of model depth in token mixing?

One interesting question is the importance of the depth of the transformer for generating representations which “mix” tokens: for instance, if there is only one layer and the parameters are random, it is unlikely for the tokens to be mixed well, whereas if there are many layers, there are many chances for the tokens to mix and form interesting representations useful for downstream tasks. We investigate this on ListOps by considering pretrained vs random models, where we only take the first X layers of the 12-layer pretrained model (i.e. for $X=3$, we use the first 3 layers of the pretrained GPT-2 model and perform classification from those hidden states). Additionally, to maximally highlight the importance of the pretrained parameters, we randomly initialize the input layer, and do not train the input or positional parameters. We first show results are finetuning the output layer and layernorm parameters, and then show only finetuning the output layer.

With finetuning layernorm. We first investigate this question with finetuning the layernorm parameters (i.e. we finetune only the output layer and the layernorm parameters). Results are shown in Table 11. Both models are unable to do well with only one layer, but the pretrained model performs significantly better than the random model at 2 layers, indicating that while the difference in performance at 12 layers is relatively small, there is a great benefit to using pretrained layers for when considering a small number of layers in that the tokens are “mixed” faster.

Number of Layers	Pretrained	Random
1	17%	17%
2	36%	16%
6	38%	35%

Table 11: Test accuracy on Listops while varying model depth and finetuning layernorm parameters. Pretrained layers “mix” the tokens faster, performing better at low model depths.

Without finetuning layernorm. We now investigate this question without finetuning the layernorm parameters, and only finetuning the output parameters, as in the reservoir computing setup in Section 3.9. Note this is equivalent to linear classification. This setting is the most challenging since all processing that is able to mix tokens is done by either random or pretrained parameters, and we are only able to train a linear layer on top of the output of the last token; as a result, the *only* token mixing that is done is performed entirely by the pretrained self-attention layers. Results are shown in Table 12. The random model does not do well even for a large number of layers, while the pretrained model can still do reasonably well, even though it requires more layers than before.

Number of Layers	Pretrained	Random
1	12%	-
3	18%	-
6	33%	-
12	33%	17%
24	-	17%

Table 12: Test accuracy on Listops while varying model depth and only training output parameters. Even for a large number of layers, the random model does not learn to perform well.

3.11 Can training more parameters improve performance?

Our focus in this work was primarily to investigate if and how efficient, general-purpose pretraining can transfer across modalities. However, for practical applications, it would naturally be more suited to choose a more specialized finetuning scheme or add more trainable parameters. In this section, we investigate additionally finetuning parameters with various methods, to see if frozen language transformers can serve as a practical base for future work.

We first investigate additionally finetuning the self-attention and feedforward layers, which were previously frozen. We simply add them to the list of parameters finetuned, without changing the

optimization or learning rate scheme, although this is suboptimal. Our results are shown in Table 13. Note that +Both is fully finetuning the 12-layer transformer (in other sections, we use full transformer to denote fully finetuning a transformer from scratch where the depth was tuned, whereas here the depth is fixed). We find that finetuning the feedforward layers can improve performance, which is similar to techniques used in prior work (Houlsby et al., 2019), but finetuning the attention layers can lead to divergence.

Model	Memory	XOR	ListOps	MNIST	C10	C10 LRA	Homology
FPT	100%	100%	38.4%	98.0%	68.2%	38.6%	12.7%
+ Feedforward	100%	100%	36.0%	98.3%	76.6%	38.2%	13.1%
+ Attention	100%	100%	36.8%	89.0% [†]	47.7% [†]	23.0%	10.9%
+ Both	100%	100%	35.8%	93.1% [†]	32.9%	21.0%	10.5%

Table 13: Additionally finetuning either the feedforward layers, attention layers, or both. We do not use a per-layer learning scheme/etc. [†]training diverged, number reported before divergence.

On CIFAR-10, we experiment with additionally finetuning the last attention layer, shown in Table 14. Generally we find smarter pretraining methods can yield better performance, so we are optimistic about the possibility of multimodal training/architectures *improving* performance in future work.

Task	Base (FPT)	+ Finetuning All FF Layers	+ Finetuning Last Attn Layer
CIFAR-10	68.2%	76.6%	80.0%

Table 14: Test accuracy on CIFAR-10 when finetuning additional parameters. In addition to FPT, if we finetune the feedforward layers and the last self-attention layer, we can achieve 80% accuracy.

3.12 Which parameters of the model are important to finetune?

We now run ablations for only finetuning select parameters to see which parameters are most sensitive. Note for all experiments (including the previous ones), we initialize the input layers as Gaussian if embeddings are used, or use an orthogonal initialization for linear layers; in particular, we find orthogonal initialization to be very important when input parameters are not trained. We highlight some results in Table 19; full results are shown on Page 16. Similar to a study of random CNNs by Frankle et al. (2020), we generally find the layer norm parameters to be most important.

Task	output only	+ layernorm	+ input	+ positions
Bit Memory	76%	94%	100%	100%
Bit XOR	56%	98%	98%	100%
ListOps	15%	36%	36%	38%
MNIST	23%	96%	98%	98%
CIFAR-10	25%	54%	60%	68%
CIFAR-10 LRA	17%	39%	39%	39%
Homology	2%	9%	10%	13%

Table 15: Ablation by successively adding certain parameters to the list of finetuned parameters for pretrained frozen transformers.

3.13 Is finetuning layer norm necessary for FPT to perform well?

While previously we showed performance gains with finetuning layer norm, we could instead consider only finetuning the input and output layers, treating the entire GPT model as a black box. We show results on CIFAR-10 in Table 16. The model performs worse; note accuracy is similar to not finetuning the positional embeddings (see Section 3.12). This suggests the internal modulation of the affine layer norm parameters help, possibly by about as much as finer positional information.

Initialization	Frozen Layer Norm	Finetuned Layer Norm
Pretrained	61.5%	68.2%
Random	55.0%	61.7%

Table 16: Test accuracy on CIFAR-10 when only finetuning the input and output layer parameters.

3.14 How well do the trends hold across other transformer models?

We also investigate how other transformer architectures perform when swapped out with GPT-2: BERT (Devlin et al., 2018), T5 (Raffel et al., 2019), and Longformer (Beltagy et al., 2020). For T5, we only use the encoder, and not the decoder. Our results are in Table 17. We find results to roughly hold across some architectures – with some differences – although T5 tends to be slightly worse than the other models. An interesting question for future work is whether subtle differences in architecture, pretraining objective, or dataset contribute to these differences.

Task	GPT-2 (FPT Default)	BERT	T5	Longformer
ListOps	38.4%	38.3%	15.4%	17.0%
CIFAR-10	68.2%	68.8%	64.7%	66.8%

Table 17: Test accuracy for frozen pretrained transformer variants (base model sizes).

4 Related Work and Discussion

4.1 Transformers in multimodal settings

Transformers (Vaswani et al., 2017) were first used successfully for natural language processing (Radford et al., 2018; Devlin et al., 2018; Radford et al., 2019; Brown et al., 2020). In recent years, they have also been shown to be effective architectures for other modalities. One particular modality of interest is computer vision (Chen et al., 2020a; Touvron et al., 2020); in particular, Dosovitskiy et al. (2020) showed that transformers can outperform CNNs in the high-data regime on standard object recognition benchmarks such as ImageNet and CIFAR. Furthermore, transformers have also been used for prediction tasks over protein sequences (Jumper et al., 2021; Rao et al., 2021), reinforcement learning (Parisotto et al., 2020), and imitation learning (Abramson et al., 2020).

Work specifically tackling multimodal tasks include Kaiser et al. (2017), who showed a single model could learn a variety of multimodal tasks with an attention architecture. Recent work has utilized transformers for multimodal predictive tasks, such as images and text in ViLBERT (Lu et al., 2019) and CLIP (Radford et al., 2021); these approaches generally use two distinct transformers to embed images and text. Lu et al. (2020) applies ViLBERT to train a single model for a variety of combined vision and language tasks. Recent work from OpenAI (Goh et al., 2021) finds that some neurons learned by CLIP are activated by a particular semantic concept, regardless of if the concept is presented in language or picture form. Our work is most similar to DALL-E (Ramesh et al., 2021), which uses a single transformer to embed both the image and text modalities, which we consider to be generating a “universal latent space” that projects any type of input into a single latent space. Such a latent space would be useful for a model that could learn from many sources of supervision.

4.2 Transformers in transfer settings

There are also many works looking at transformers specifically in the context of in-modality transfer, such as ViT for vision (Dosovitskiy et al., 2020), T5 for language (Raffel et al., 2019), and UDSMProt for protein sequences (Strodthoff et al., 2020). CLIP (Radford et al., 2021) showed that training on text in addition to images could allow for zero-shot classification via providing downstream labels as text. Hernandez et al. (2021) do a thorough investigation of transfer with language pretraining, notably showing transfer from English to Python, which they consider to be reasonably distanced from English; many works have also looked at transferring from one language to another (Artetxe et al., 2019; Ponti et al., 2019). Similar to our work, Papadimitriou & Jurafsky (2020)

investigate transfer for LSTMs between modalities including code, different languages, and music, finding that pretraining on “non-linguistic data with latent structure” can transfer to language, finding grammatical structure in a modality to be important, although we generally investigate the other direction and explore more distanced modalities. Kiela et al. (2019) make similar observations for aligning representation spaces of language and vision. Li et al. (2020) pretrain on a referential communication game where an emergent learned language is used to transfer to NLP tasks. Wu et al. (2021) found explicitly pretraining computational primitives to transfer to mathematics tasks.

4.3 Pretraining and finetuning of transformer models

A common trend in deep learning models is to first train a large model on an unsupervised objective on a large dataset (Dai & Le, 2015; Radford et al., 2018) and then finetune on a small downstream dataset (e.g., by freezing the model and only finetuning the output layer). A common method used to finetune transformers are adapter networks (Rebuffi et al., 2017; Houtsby et al., 2019), which add a fully connected residual block for each unique downstream task and also finetune the layer norm parameters. For simplicity, we do not add the full adapter block but only train the layer norm parameters, reducing the number of parameters we consider. These techniques used are similar to prior approaches such as FiLM (Perez et al., 2018) and self-modulation (Chen et al., 2018). A recent direction of research has explored learning prompt templates for large models (Shin et al., 2020) that simply require forward passes over the transformer. Unlike these works, we consider finetuning on one modality (language) and finetuning on others, whereas prior work investigates finetuning on the same modality as the pretraining task. Another interesting related work, although not investigating transformers, by Frankle et al. (2020) find randomly initialized CNNs, which only train the batchnorm affine parameters, to work well on CIFAR-10. Their numbers are stronger than ours on CIFAR-10, but include significantly more inductive bias via a convolutional architecture, so the main takeaway is slightly more relevant towards image tasks rather than arbitrary sequences.

4.4 Self-attention layers as optimization steps

The nature of computation performed by self-attention layers has also been explored by other related works. Bai et al. (2019) show that a single transformer self-attention block can be trained to perform an optimization step towards finding a stationary point, representing the solution to the task. Ramsauer et al. (2020) show that the self-attention layer is a gradient step in a Hopfield network with a learning rate of 1, hinting that transformers are capable of storing and retrieving a large amount of patterns with an implicit energy function. An interesting discussion from Goyal & Bengio (2020) points out a connection in viewing the key-value queries used in attention as similar to function signatures in computer programming: the key maps the input to a type (e.g., float) and the value maps the input to its value (e.g., 3.14), and if the type matches the function signature, the function can be applied to the value – this may be particularly relevant when we consider using a single self-attention layer applied to different modalities, as the modality may be embedded in the type.

4.5 Global workspace theory

A common technique for evaluating the embeddings learned by an unsupervised model is to train a linear layer on top of the embeddings for a downstream task (Donahue et al., 2016; Oord et al., 2018; Chen et al., 2020b), which is reasonable when you finetune on the same modality as the pretrained one. However, when finetuning on a different modality, as in our setting, we have to reframe this notion of generalizable embedding quality – instead of only finetuning the output layer, we also want to finetune the input layer, and instead evaluate the ability of the frozen intermediate model to perform generalizable *computation*. This is reminiscent of Global Workspace Theory (Baars, 1993), which revolves around the notion that there is a “blackboard” that different parts of the brain send data to; we might consider the frozen language model as being a blackboard in this setting. Language might also be a natural choice of model for this blackboard, as there are hypotheses that language may serve as a good multipurpose high-level representation for cognitive behavior and conscious planning (Andreas et al., 2017; Goyal & Bengio, 2020).

4.6 Reservoir computing

Similarly to the FPT setup and Global Workspace Theory, in reservoir computing (Tanaka et al., 2019) and echo state networks (Jaeger, 2001; Jaeger & Haas, 2004), a random recurrent network is frozen and only the output readout layer is trained. These models are very fast to train, using a similar setup as in Section 3.9, because the activations of the recurrent network can be cached and it is unnecessary to backpropagate over time. Somewhat differently to the FPT architecture, echo state networks are recurrent and thus feed back into themselves, which allows the outputs of the random frozen network to modulate future inputs. Unlike echo state networks, we also notably finetune the input and positional embeddings, which allow the inputs to the frozen network to adapt to a particular modality/for a query to the frozen network to be learned. Echo state networks are also similar to the perspective of self-attention applying a data-dependent filter to the inputs, as opposed to 1D convolutions, which are fixed filters regardless of the input modality.

5 Conclusion

We proposed transferring a pretrained transformer language model for downstream tasks in non-language modalities. Through extensive empirical evaluation, we showed that these models could achieve performance competitive with transformers fully trained on the downstream task without having to finetune the self-attention and feedforward layers, relying solely on frozen parameters from the language model to perform the bulk of the computation.

We believe this work can serve as the foundation for future work investigating transfer between modalities. In future, we are interested in investigating the use of other data-rich modalities (e.g., vision) or a hybrid of multiple domains being used to provide the necessary substrate for pretraining a universal computational engine. It would also be interesting to explore frozen pretrained models for tasks beyond predictive modeling, such as reinforcement learning (Abramson et al., 2020).

We note that a limitation of our analysis is that we analyze specific models on a restricted set of tasks. More investigation can highlight whether or not similar behavior occurs for other models on other tasks. For instance, in Section 3.14, we find the architecture can have a significant impact on results. As training regimes for these models evolve, performing similar experiments may yield different results, and we are excited for more research in this direction.

For high stakes applications in the real-world, there are potential concerns with transfer of harmful biases from one modality to one another using pretrained transformer models trained on vast quantities of unlabeled, uncurated datasets (Sheng et al., 2019; Bender et al., 2021). Mitigating these biases is an active area of research (Grover et al., 2019; Choi et al., 2020). Conversely, there are also potential upsides with FPT models being able to better exploit representative datasets from one or more modalities, which merit future investigation as well.

Acknowledgements

We would like to thank Luke Metz, Kimin Lee, Fangchen Liu, Roshan Rao, Aravind Srinivas, Nikita Kitaev, Daniel Freeman, Marc’Aurelio Ranzato, Jacob Andreas, and Ashish Vaswani for valuable feedback and discussions. We would also like to thank members of the community for providing feedback online on an earlier version of this paper.

Parameter ablations for pretrained models

Task	output only	output + input	output + positions	output + layernorm
Bit Memory	76%	98%	93%	94%
Bit XOR	56%	72%	84%	98%
ListOps	15%	17%	35%	36%
MNIST	23%	85%	93%	96%
CIFAR-10	25%	53%	38%	54%
CIFAR-10 LRA	17%	22%	30%	39%
Homology	2%	8%	8%	9%

Table 18: Ablation by only finetuning individual types of parameters for pretrained frozen transformers. We bold the most important parameter (measured by highest test accuracy) for each task.

Task	output only	+ layernorm	+ input	+ positions
Bit Memory	76%	94%	100%	100%
Bit XOR	56%	98%	98%	100%
ListOps	15%	36%	36%	38%
MNIST	23%	96%	98%	98%
CIFAR-10	25%	54%	60%	68%
CIFAR-10 LRA	17%	39%	39%	39%
Homology	2%	9%	10%	13%

Table 19: Ablation by successively adding certain parameters to the list of finetuned parameters for pretrained frozen transformers.

Parameter ablations for random models

Task	output only	output + input	output + positions	output + layernorm
Bit Memory	75%	75%	75%	75%
Bit XOR	50%	51%	59%	100%
ListOps	17%	17%	18%	35%
MNIST	25%	28%	34%	83%
CIFAR-10	20%	24%	21%	46%
CIFAR-10 LRA	11%	16%	12%	34%
Homology	2%	2%	6%	9%

Table 20: Finetuning individual types of parameters for random frozen transformers.

Task	output only	+ layernorm	+ input	+ positions
Bit Memory	75%	75%	75%	76%
Bit XOR	50%	100%	100%	100%
ListOps	17%	35%	36%	37%
MNIST	25%	83%	92%	92%
CIFAR-10	20%	46%	56%	62%
CIFAR-10 LRA	11%	34%	36%	36%
Homology	2%	9%	9%	9%

Table 21: Ablation by successively adding certain parameters to the list of finetuned parameters for random frozen transformers.

References

- Josh Abramson, Arun Ahuja, Arthur Brussee, Federico Carnevale, Mary Cassin, Stephen Clark, Andrew Dudzik, Petko Georgiev, Aurelia Guy, Tim Harley, et al. Imitating interactive intelligence. *arXiv preprint arXiv:2012.05672*, 2020.
- Jacob Andreas, Dan Klein, and Sergey Levine. Learning with latent language. *arXiv preprint arXiv:1711.00482*, 2017.
- Mikel Artetxe, Sebastian Ruder, and Dani Yogatama. On the cross-lingual transferability of monolingual representations. *arXiv preprint arXiv:1910.11856*, 2019.
- Jimmy Lei Ba, Jamie Ryan Kiros, and Geoffrey E Hinton. Layer normalization. *arXiv preprint arXiv:1607.06450*, 2016.
- Bernard J Baars. *A cognitive theory of consciousness*. Cambridge University Press, 1993.
- Shaojie Bai, J Zico Kolter, and Vladlen Koltun. Deep equilibrium models. *arXiv preprint arXiv:1909.01377*, 2019.
- Iz Beltagy, Matthew E Peters, and Arman Cohan. Longformer: The long-document transformer. *arXiv preprint arXiv:2004.05150*, 2020.
- Emily M Bender, Timnit Gebru, Angelina McMillan-Major, and Shmargaret Shmitchell. On the dangers of stochastic parrots: Can language models be too big. In *Proceedings of the 2020 Conference on Fairness, Accountability, and Transparency; Association for Computing Machinery: New York, NY, USA*, 2021.
- Tom B Brown, Benjamin Mann, Nick Ryder, Melanie Subbiah, Jared Kaplan, Prafulla Dhariwal, Arvind Neelakantan, Pranav Shyam, Girish Sastry, Amanda Askell, et al. Language models are few-shot learners. *arXiv preprint arXiv:2005.14165*, 2020.
- Mark Chen, Alec Radford, Rewon Child, Jeffrey Wu, Heewoo Jun, David Luan, and Ilya Sutskever. Generative pretraining from pixels. In *International Conference on Machine Learning*, pp. 1691–1703. PMLR, 2020a.
- Ting Chen, Mario Lucic, Neil Houlsby, and Sylvain Gelly. On self modulation for generative adversarial networks. *arXiv preprint arXiv:1810.01365*, 2018.
- Ting Chen, Simon Kornblith, Mohammad Norouzi, and Geoffrey Hinton. A simple framework for contrastive learning of visual representations. In *International conference on machine learning*, pp. 1597–1607. PMLR, 2020b.
- Kristy Choi, Aditya Grover, Trisha Singh, Rui Shu, and Stefano Ermon. Fair generative modeling via weak supervision. In *International Conference on Machine Learning*, pp. 1887–1898. PMLR, 2020.
- Andrew M Dai and Quoc V Le. Semi-supervised sequence learning. *arXiv preprint arXiv:1511.01432*, 2015.
- Jia Deng, Wei Dong, Richard Socher, Li-Jia Li, Kai Li, and Li Fei-Fei. Imagenet: A large-scale hierarchical image database. In *2009 IEEE conference on computer vision and pattern recognition*, pp. 248–255. Ieee, 2009.
- Jacob Devlin, Ming-Wei Chang, Kenton Lee, and Kristina Toutanova. Bert: Pre-training of deep bidirectional transformers for language understanding. *arXiv preprint arXiv:1810.04805*, 2018.
- Jeff Donahue, Philipp Krähenbühl, and Trevor Darrell. Adversarial feature learning. *arXiv preprint arXiv:1605.09782*, 2016.
- Alexey Dosovitskiy, Lucas Beyer, Alexander Kolesnikov, Dirk Weissenborn, Xiaohua Zhai, Thomas Unterthiner, Mostafa Dehghani, Matthias Minderer, Georg Heigold, Sylvain Gelly, et al. An image is worth 16x16 words: Transformers for image recognition at scale. *arXiv preprint arXiv:2010.11929*, 2020.

- Sara El-Gebali, Jaina Mistry, Alex Bateman, Sean R Eddy, Aurélien Luciani, Simon C Potter, Matloob Qureshi, Lorna J Richardson, Gustavo A Salazar, Alfredo Smart, Erik L L Sonnhammer, Layla Hirsh, Lisanna Paladin, Damiano Piovesan, Silvio C E Tosatto, and Robert D Finn. The Pfam protein families database in 2019. *Nucleic Acids Research*, 47(D1):D427–D432, 2019. ISSN 0305-1048. doi: 10.1093/nar/gky995.
- Naomi K Fox, Steven E Brenner, and John-Marc Chandonia. Scope: Structural classification of proteins—extended, integrating scop and astral data and classification of new structures. *Nucleic acids research*, 42(D1):D304–D309, 2013.
- Jonathan Frankle, David J Schwab, and Ari S Morcos. Training batchnorm and only batchnorm: On the expressive power of random features in cnns. *arXiv preprint arXiv:2003.00152*, 2020.
- Gabriel Goh, Chelsea Voss, Daniela Amodei, Shan Carter, Michael Petrov, Justin Jay Wang, Nick Cammarata, and Chris Olah. Multimodal neurons in artificial neural networks. 2021.
- Anirudh Goyal and Yoshua Bengio. Inductive biases for deep learning of higher-level cognition. *arXiv preprint arXiv:2011.15091*, 2020.
- Aditya Grover, Jiaming Song, Alekh Agarwal, Kenneth Tran, Ashish Kapoor, Eric Horvitz, and Stefano Ermon. Bias correction of learned generative models using likelihood-free importance weighting. *arXiv preprint arXiv:1906.09531*, 2019.
- Kaiming He, Xiangyu Zhang, Shaoqing Ren, and Jian Sun. Deep residual learning for image recognition. In *Proceedings of the IEEE conference on computer vision and pattern recognition*, pp. 770–778, 2016.
- Dan Hendrycks and Kevin Gimpel. Gaussian error linear units (gelus). *arXiv preprint arXiv:1606.08415*, 2016.
- Danny Hernandez, Jared Kaplan, Tom Henighan, and Sam McCandlish. Scaling laws for transfer. *arXiv preprint arXiv:2102.01293*, 2021.
- Sepp Hochreiter and Jürgen Schmidhuber. Long short-term memory. *Neural computation*, 9(8):1735–1780, 1997.
- Jie Hou, Badri Adhikari, and Jianlin Cheng. Deepsf: deep convolutional neural network for mapping protein sequences to folds. *Bioinformatics*, 34(8):1295–1303, 2018.
- Neil Houlsby, Andrei Giurgiu, Stanislaw Jastrzebski, Bruna Morrone, Quentin De Laroussilhe, Andrea Gesmundo, Mona Attariyan, and Sylvain Gelly. Parameter-efficient transfer learning for nlp. In *International Conference on Machine Learning*, pp. 2790–2799. PMLR, 2019.
- Herbert Jaeger. The “echo state” approach to analysing and training recurrent neural networks—with an erratum note. *Bonn, Germany: German National Research Center for Information Technology GMD Technical Report*, 148(34):13, 2001.
- Herbert Jaeger and Harald Haas. Harnessing nonlinearity: Predicting chaotic systems and saving energy in wireless communication. *science*, 304(5667):78–80, 2004.
- John Jumper, Richard Evans, Alexander Pritzel, Tim Green, Michael Figurnov, Kathryn Tunyasuvunakool, Olaf Ronneberger, Russ Bates, Augustin Žídek, Alex Bridgland, Clemens Meyer, Simon A A Kohl, Anna Potapenko, Andrew J Ballard, Andrew Cowie, Bernardino Romera-Paredes, Stanislav Nikolov, Rishub Jain, Jonas Adler, Trevor Back, Stig Petersen, David Reiman, Martin Steinegger, Michalina Pacholska, David Silver, Oriol Vinyals, Andrew W Senior, Koray Kavukcuoglu, Pushmeet Kohli, and Demis Hassabis. High accuracy protein structure prediction using deep learning. 2021.
- Lukasz Kaiser, Aidan N Gomez, Noam Shazeer, Ashish Vaswani, Niki Parmar, Llion Jones, and Jakob Uszkoreit. One model to learn them all. *arXiv preprint arXiv:1706.05137*, 2017.
- Douwe Kiela, Suvrat Bhooshan, Hamed Firooz, Ethan Perez, and Davide Testuggine. Supervised multimodal bitransformers for classifying images and text. *arXiv preprint arXiv:1909.02950*, 2019.

- Diederik P Kingma and Jimmy Ba. Adam: A method for stochastic optimization. *arXiv preprint arXiv:1412.6980*, 2014.
- Alex Krizhevsky et al. Learning multiple layers of features from tiny images. 2009.
- Yaoyiran Li, Edoardo M Ponti, Ivan Vulić, and Anna Korhonen. Emergent communication pretraining for few-shot machine translation. *arXiv preprint arXiv:2011.00890*, 2020.
- Jiasen Lu, Dhruv Batra, Devi Parikh, and Stefan Lee. Vilbert: Pretraining task-agnostic visiolinguistic representations for vision-and-language tasks. *arXiv preprint arXiv:1908.02265*, 2019.
- Jiasen Lu, Vedanuj Goswami, Marcus Rohrbach, Devi Parikh, and Stefan Lee. 12-in-1: Multi-task vision and language representation learning. In *Proceedings of the IEEE/CVF Conference on Computer Vision and Pattern Recognition*, pp. 10437–10446, 2020.
- Thomas Miconi, Kenneth Stanley, and Jeff Clune. Differentiable plasticity: training plastic neural networks with backpropagation. In *International Conference on Machine Learning*, pp. 3559–3568. PMLR, 2018.
- Aaron van den Oord, Yazhe Li, and Oriol Vinyals. Representation learning with contrastive predictive coding. *arXiv preprint arXiv:1807.03748*, 2018.
- Isabel Papadimitriou and Dan Jurafsky. Pretraining on non-linguistic structure as a tool for analyzing learning bias in language models. *arXiv preprint arXiv:2004.14601*, 2020.
- Emilio Parisotto, Francis Song, Jack Rae, Razvan Pascanu, Caglar Gulcehre, Siddhant Jayakumar, Max Jaderberg, Raphael Lopez Kaufman, Aidan Clark, Seb Noury, et al. Stabilizing transformers for reinforcement learning. In *International Conference on Machine Learning*, pp. 7487–7498. PMLR, 2020.
- Adam Paszke, Sam Gross, Francisco Massa, Adam Lerer, James Bradbury, Gregory Chanan, Trevor Killeen, Zeming Lin, Natalia Gimelshein, Luca Antiga, et al. Pytorch: An imperative style, high-performance deep learning library. *arXiv preprint arXiv:1912.01703*, 2019.
- Ethan Perez, Florian Strub, Harm De Vries, Vincent Dumoulin, and Aaron Courville. Film: Visual reasoning with a general conditioning layer. In *Proceedings of the AAAI Conference on Artificial Intelligence*, volume 32, 2018.
- Edoardo Maria Ponti, Ivan Vulić, Ryan Cotterell, Roi Reichart, and Anna Korhonen. Towards zero-shot language modeling. In *Proceedings of the 2019 Conference on Empirical Methods in Natural Language Processing and the 9th International Joint Conference on Natural Language Processing (EMNLP-IJCNLP)*, pp. 2893–2903, 2019.
- Alec Radford, Karthik Narasimhan, Tim Salimans, and Ilya Sutskever. Improving language understanding by generative pre-training. 2018.
- Alec Radford, Jeffrey Wu, Rewon Child, David Luan, Dario Amodei, and Ilya Sutskever. Language models are unsupervised multitask learners. 2019.
- Alec Radford, Jong Wook Kim, Chris Hallacy, Aditya Ramesh, Gabriel Goh, Sandhini Agarwal, Girish Sastry, Amanda Askell, Pamela Mishkin, Jack Clark, et al. Learning transferable visual models from natural language supervision. *Image*, 2:T2, 2021.
- Colin Raffel, Noam Shazeer, Adam Roberts, Katherine Lee, Sharan Narang, Michael Matena, Yanqi Zhou, Wei Li, and Peter J Liu. Exploring the limits of transfer learning with a unified text-to-text transformer. *arXiv preprint arXiv:1910.10683*, 2019.
- Aditya Ramesh, Mikhail Pavlov, Gabriel Goh, Scott Gray, Mark Chen, Rewon Child, Vedant Misra, Pamela Mishkin, Gertchen Krueger, Sandhini Agarwal, and Ilya Sutskever. Dall-e: Creating images from text, 2021.
- Hubert Ramsauer, Bernhard Schäfl, Johannes Lehner, Philipp Seidl, Michael Widrich, Lukas Gruber, Markus Holzleitner, Milena Pavlović, Geir Kjetil Sandve, Victor Greiff, et al. Hopfield networks is all you need. *arXiv preprint arXiv:2008.02217*, 2020.

- Roshan Rao, Nicholas Bhattacharya, Neil Thomas, Yan Duan, Xi Chen, John Canny, Pieter Abbeel, and Yun S Song. Evaluating protein transfer learning with tape. In *Advances in Neural Information Processing Systems*, 2019.
- Roshan Rao, Jason Liu, Robert Verkuil, Joshua Meier, John F. Canny, Pieter Abbeel, Tom Sercu, and Alexander Rives. Msa transformer. *bioRxiv*, 2021. doi: 10.1101/2021.02.12.430858.
- Sylvestre-Alvise Rebuffi, Hakan Bilen, and Andrea Vedaldi. Learning multiple visual domains with residual adapters. *arXiv preprint arXiv:1705.08045*, 2017.
- David E Rumelhart, Geoffrey E Hinton, and Ronald J Williams. Learning internal representations by error propagation. Technical report, California Univ San Diego La Jolla Inst for Cognitive Science, 1985.
- Emily Sheng, Kai-Wei Chang, Premkumar Natarajan, and Nanyun Peng. The woman worked as a babysitter: On biases in language generation. *arXiv preprint arXiv:1909.01326*, 2019.
- Taylor Shin, Yasaman Razeghi, Robert L Logan IV, Eric Wallace, and Sameer Singh. Autoprompt: Eliciting knowledge from language models with automatically generated prompts. *arXiv preprint arXiv:2010.15980*, 2020.
- Nils Strodthoff, Patrick Wagner, Markus Wenzel, and Wojciech Samek. Udsmprot: universal deep sequence models for protein classification. *Bioinformatics*, 36(8):2401–2409, 2020.
- Gouhei Tanaka, Toshiyuki Yamane, Jean Benoit Héroux, Ryosho Nakane, Naoki Kanazawa, Seiji Takeda, Hidetoshi Numata, Daiju Nakano, and Akira Hirose. Recent advances in physical reservoir computing: A review. *Neural Networks*, 115:100–123, 2019.
- Yi Tay, Mostafa Dehghani, Samira Abnar, Yikang Shen, Dara Bahri, Philip Pham, Jinfeng Rao, Liu Yang, Sebastian Ruder, and Donald Metzler. Long range arena: A benchmark for efficient transformers. *arXiv preprint arXiv:2011.04006*, 2020.
- Hugo Touvron, Matthieu Cord, Matthijs Douze, Francisco Massa, Alexandre Sablayrolles, and Hervé Jégou. Training data-efficient image transformers & distillation through attention. *arXiv preprint arXiv:2012.12877*, 2020.
- Ashish Vaswani, Noam Shazeer, Niki Parmar, Jakob Uszkoreit, Llion Jones, Aidan N Gomez, Lukasz Kaiser, and Illia Polosukhin. Attention is all you need. *arXiv preprint arXiv:1706.03762*, 2017.
- Ross Wightman. Pytorch image models. <https://github.com/rwightman/pytorch-image-models>, 2019.
- Thomas Wolf, Lysandre Debut, Victor Sanh, Julien Chaumond, Clement Delangue, Anthony Moi, Pierric Cistac, Tim Rault, Rémi Louf, Morgan Funtowicz, Joe Davison, Sam Shleifer, Patrick von Platen, Clara Ma, Yacine Jernite, Julien Plu, Canwen Xu, Teven Le Scao, Sylvain Gugger, Mariama Drame, Quentin Lhoest, and Alexander M. Rush. Transformers: State-of-the-art natural language processing. In *Proceedings of the 2020 Conference on Empirical Methods in Natural Language Processing: System Demonstrations*, pp. 38–45, Online, October 2020. Association for Computational Linguistics.
- Yuhuai Wu, Markus Rabe, Wenda Li, Jimmy Ba, Roger Grosse, and Christian Szegedy. Lime: Learning inductive bias for primitives of mathematical reasoning. *arXiv preprint arXiv:2101.06223*, 2021.

Appendix

Contents

A	Summary of arXiv Updates	22
B	Background on Transformers	22
B.1	Self-Attention	22
B.2	Positional Embeddings	22
B.3	Layer Norm	23
B.4	Pretraining Objective	23
B.5	Model Sizes	23
C	Experimental Details	23
D	Details by Table	24
D.1	Can pretrained language models transfer to different modalities?	24
D.2	What is the importance of the pretraining modality?	25
D.3	How important is the transformer architecture compared to LSTM architecture? . .	25
D.4	Does language pretraining improve compute efficiency over random initialization?	26

A Summary of arXiv Updates

We summarize changes made in updated versions:

- v1. (9 Mar 2021) Original release.
- v2. (30 June 2021) Updated Section 3.3 with more analysis of the frozen LSTM architecture and additional experimental details. Added new Section 3.10 discussing model depth and token mixing, new results in Section 3.11 discussing how different freezing strategies can improve performance, and attention mask visualization for random frozen transformer to Section 3.5. Included more details about experiments and hyperparameters, and added some new citations (notably Wu et al. (2021) for related LIME work and Frankle et al. (2020) for similar frozen analysis for CNNs). Github was also updated to include LSTM architecture, vision pretraining, and remote homology tasks. Minor writing updates.

B Background on Transformers

In this section, we give a description of the transformer architecture used in our experiments, namely the GPT-2 architecture (Radford et al., 2019).

B.1 Self-Attention

The main subcomponent of the transformer architecture is the self-attention layer, which takes in l input tokens and outputs l output tokens, both of dimension n_{dim} . Each input token x_i is mapped by linear transformations Q , K , and V – denoting query, key, and values, respectively – into q_i , k_i , and v_i . Both q_i and k_i have dimension d_k , and v_i has dimension d_v . To generate the output token y_i , dot products are calculated between query q_i and keys k_j , and fed into a softmax operation to generate weights $w_i \in [0, 1]$ (in practice, a scaling temperature factor of $\frac{1}{\sqrt{d_k}}$ is used to reduce the sharpness of the softmax). Then, the weights are used to generate y_i as a weighted sum of all the values, i.e.:

$$y_i = \sum_{j=1}^l \frac{\exp(q_i^\top k_j)}{\sum_{k=1}^l \exp(q_i^\top k_k)} v_j \quad (1)$$

This is extended to *multi-head* attention over n_{heads} heads by doing the above procedure n_{heads} times, and then concatenating. To recover the original dimension the concatenated vector (of dimension $d_v n_{heads}$) is multiplied by a projection matrix $W_{proj} \in \mathbb{R}^{d_v n_{heads} \times n_{dim}}$.

GPT-2 applies a causal mask to its inputs, i.e. the output token i is only allowed to attend to the input tokens $j \leq i$, which changes the upper bounds of the sums in Equation 1 to i instead of l . This allows for unsupervised pretraining methods like language modeling (see Appendix B.4).

A residual connection is used to connect the inputs with the outputs of the attention layer. Then, in the rest of the transformer block, a two-layer MLP is used, conventionally projecting the dimension upwards to $4 \cdot n_{dim}$ for the inner dimension and using the GELU activation function (Hendrycks & Gimpel, 2016). Another residual connection is used to connect the outputs of the MLP with the previous outputs of the attention layer.

This forms the basis of the transformer block. As it preserves the dimension n_{dim} , multiple blocks can be learned and stacked on top of each other n_{layers} times, before feeding the final hidden states to the output layer. In our work, we only use the output of the last hidden state for classification, although in principle other methods are reasonable.

B.2 Positional Embeddings

As the self-attention blocks are permutation-invariant, in order to capture positional information about sequences, positional embeddings are learned. For each position $i \in (1, \dots, \text{max_len})$, a vector p_i is learned. At the front of the transformer, before feeding in the inputs x_i into the self-attention blocks, the positional embeddings are added to the input embeddings as $x_i := x_i + p_i$.

B.3 Layer Norm

Layer norm (Ba et al., 2016) is frequently used in recurrent and transformer architectures as a means of normalizing the activations. In particular, for the activations of training example x of dimension n_{dim} , it normalizes by the mean and variance over the features:

$$\tilde{y}_i = \frac{x_i - \text{mean}(\{x_j\}_{j=1}^{n_{dim}})}{\text{std}(\{x_j\}_{j=1}^{n_{dim}})} \quad (2)$$

Then, affine scale and shift parameters each of dimension $n_{dim} - \gamma$ and β , respectively – are learned to generate the outputs y .

$$y_i = \gamma_i \tilde{y}_i + \beta_i \quad (3)$$

Layer norm is applied twice per self-attention block: once before the attention layer and once before the MLP. As a result, a total of $4 \cdot n_{layers} \cdot n_{dim}$ layer norm parameters are learned.

B.4 Pretraining Objective

GPT-2 is pretrained on an autoregressive language modeling objective optimizing for parameters which maximize the log-likelihood of the data: $\max_{\theta} \mathbb{E}[\log p_{\theta}(x)]$. GPT-2 models sequences autoregressively, factorizing the probability distribution $p(x) = p(x_1, \dots, x_l)$ via chain rule as:

$$p(x) = \prod_{i=1}^l p(x_i | x_{i-1}, \dots, x_1) \quad (4)$$

For the language domain, this objective can be interpreted as “given the previous $i - 1$ words of a sentence, predict the next word”.

B.5 Model Sizes

The model sizes from Section 3.7 are as follows:

Model Size	n_{layers}	n_{dim}	n_{heads}	# Parameters
Small (Base)	12	768	12	117M
Medium	24	1024	16	345M
Large	36	1280	20	774M

Table 22: Hyperparameters for architectures for larger model sizes.

The hyperparameters for the experiments with other architectures (Vision Transformer, BERT, Longformer, T5) are the same as for the base model size shown above.

C Experimental Details

We use implementations of and pretrained models from the Huggingface Transformers library (Wolf et al., 2020). We train all models using the Adam (Kingma & Ba, 2014) optimizer following Pytorch (Paszke et al., 2019) defaults. For all transformer models, we use a learning rate of 10^{-3} without learning rate scheduling. For the remote homology task only, we use a learning rate of 10^{-4} as we found it to give better performance than 10^{-3} . We generally use the largest batch size that fits on an RTX 2080 Ti graphics card, somewhere between 2 and 16, without gradient accumulation. Note that except for the remote homology task, we did not tune the FPT hyperparameters. For all LSTMs, we use a lower learning rate of 3×10^{-4} and the same batch sizes as transformers of the same size. Models are trained to convergence and evaluated on a heldout test set.

D Details by Table

For clarity, we explicitly write out finer details for some experiment sections where numbers can represent different model types.

D.1 Can pretrained language models transfer to different modalities?

This section refers to Table 1 in Section 3.1.

Bit Memory

1. FPT: 12-layer base size FPT model (finetuning input, output, position, and layernorm params).
2. Full: 12-layer base size GPT-2 model (training all params).
3. LSTM: 3-layer, 768 hidden dimension LSTM model (training all params).

Bit XOR

1. FPT: 12-layer base size FPT model (finetuning input, output, position, and layernorm params).
2. Full: 12-layer base size GPT-2 model (training all params).
3. LSTM: 3-layer, 768 hidden dimension LSTM model (training all params).

ListOps

1. FPT: 12-layer base size FPT model (finetuning input, output, position, and layernorm params).
2. Full: number reported from Tay et al. (2020) (3-layer vanilla transformer).
3. LSTM: 3-layer, 768 hidden dimension LSTM model (training all params).

CIFAR-10

1. FPT: 36-layer large size FPT model (finetuning input, output, position, and layernorm params).
2. Full: 3-layer, 768 hidden dimension GPT-2 model (training all params).
3. LSTM: 3-layer, 768 hidden dimension LSTM model (training all params).

CIFAR-10 LRA

1. FPT: 12-layer base size FPT model (finetuning input, output, position, and layernorm params).
2. Full: number reported from Tay et al. (2020) (3-layer vanilla transformer).
3. LSTM: 3-layer, 768 hidden dimension LSTM model (training all params).

Remote Homology

1. FPT: 12-layer base size FPT model (finetuning input, output, position, and layernorm params).
2. Full: number reported from Rao et al. (2019) (12-layer, 512 hidden dimension vanilla transformer).
3. LSTM: 3-layer, 768 hidden dimension LSTM model (training all params).

D.2 What is the importance of the pretraining modality?

This section refers to Table 2 in Section 3.2.

All tasks

1. FPT: 12-layer base size FPT model (finetuning input, output, position, and layernorm params). This differs from Table 1, Section 3.1 only in the CIFAR-10 model size.
2. Random: 12-layer randomly initialized (default scheme) base size GPT-2 model (training input, output, position, and layernorm params).
3. Bit: 12-layer base size GPT-2 model (finetuning input, output, position, and layernorm params), after first being fully finetuned on Bit Memory following default random initialization.
4. ViT: 12-layer, 768 hidden dimension base size ViT model (finetuning input, output, position, and layernorm params), pretrained on 224×224 ImageNet-21k with a patch size of 16. (`vit_base_patch16_224` from the `timm` Pytorch library (Wightman, 2019)). We reinitialize the input layer from scratch to match each task, and do not use a CLS token or an MLP as the output network – instead using a linear layer from the last token – matching the protocol for the other methods.

D.3 How important is the transformer architecture compared to LSTM architecture?

The following refer to Section 3.3. In Table 3:

All tasks

1. Trans: 12-layer randomly initialized (default scheme) base size GPT-2 model (training input, output, and layernorm params). Note: same as “Random” in Table 2, Section 3.2.
2. LSTM: 3-layer, 768 hidden dimension “standard” LSTM (training input, output, and layernorm params). Does not have residual connections or positional embeddings.
3. LSTM*: 12-layer, 768 hidden dimension LSTM (training input, output, position, and layernorm params).

Table 4:

All tasks

1. 12: 12-layer, 768 hidden dimension “standard” LSTM (training input, output, and layernorm params).
2. 3: 3-layer, 768 hidden dimension “standard” LSTM (training input, output, and layernorm params).

Table 5:

All tasks

1. 12-layer LSTM: 12-layer, 768 hidden dimension “standard” LSTM (training input, output, and layernorm params). Note: same as “12” in Table 4, Section 3.3.
2. + Residual Connections: 12-layer, 768 hidden dimension LSTM with residual connections (training input, output, and layernorm params).
3. + Positional Embeddings: 12-layer, 768 hidden dimension LSTM with residual connections and positional embeddings (training input, output, position, and layernorm params). Note: same as “LSTM*” in Table 3, Section 3.3.

D.4 Does language pretraining improve compute efficiency over random initialization?

This section refers to Table 6 in Section 3.4.

All tasks

1. FPT: 12-layer base size FPT model (finetuning input, output, position, and layernorm params). Note: same models as “FPT” in Table 2, Section 3.2.
2. Random: 12-layer randomly initialized (default scheme) base size GPT-2 model (training input, output, position, and layernorm params). Note: same models as “Random” in Table 2, Section 3.2.